Intensity estimation for spatial point processes observed with noise

Lionel Cucala

METMA

September 2006

Outline

- Perturbed point processes.
- The deconvolution method.
- An asymptotic study.
- The bandwidth selection procedure.
- A simulation study.

Perturbed point processes

Perturbed point processes

- $\mathbf{Y}$ point process defined on $X \subseteq \mathbb{R}^2$.

Perturbed point processes

- $\mathbf{Y}$ point process defined on $X \subseteq \mathbb{R}^2$.
- We observe $Z = \{z_1, \cdots, z_n\}$ on the bounded domain $D \subseteq X$ such that

Perturbed point processes

- $\mathbf{Y}$ point process defined on $X \subseteq \mathbb{R}^2$.
- We observe $Z = \{z_1, \cdots, z_n\}$ on the bounded domain $D \subseteq X$ such that

$$z_i = y_i + \epsilon_i, \quad i = 1, \cdots, n$$

Perturbed point processes

- $\mathbf{Y}$ point process defined on $X \subseteq \mathbb{R}^2$.
- We observe $Z = \{z_1, \cdots, z_n\}$ on the bounded domain $D \subseteq X$ such that

$$z_i = y_i + \epsilon_i, \quad i = 1, \cdots, n$$

$$\{\epsilon_i, \ i = 1, \cdots, n\} \ i.i.d. \sim g(.)$$

Perturbed point processes

- $\mathbf{Y}$ point process defined on $X \subseteq \mathbb{R}^2$.
- We observe $Z = \{z_1, \cdots, z_n\}$ on the bounded domain $D \subseteq X$ such that

$$z_i = y_i + \epsilon_i, \quad i = 1, \cdots, n$$

$$\{\epsilon_i,\ i = 1, \cdots, n\}\ i.i.d. \sim g(.)$$

$$\epsilon_i \perp\!\!\!\perp y_i, \quad i = 1, \cdots, n$$

Perturbed point processes

- $\mathbf{Y}$ point process defined on $X \subseteq \mathbb{R}^2$.
- We observe $Z = \{z_1, \cdots, z_n\}$ on the bounded domain $D \subseteq X$ such that

$$z_i = y_i + \epsilon_i, \quad i = 1, \cdots, n$$

$$\{\epsilon_i, \;\; i = 1, \cdots, n\} \;\; i.i.d. \sim g(.)$$

$$\epsilon_i \perp\!\!\!\perp y_i, \quad i = 1, \cdots, n$$

- Goal: estimate $\lambda_Y(s)$ for every point $s \in D$.

Kernel intensity estimator

Kernel intensity estimator

Diggle (1985):

Kernel intensity estimator

Diggle (1985):

$$\forall s \in \mathbb{R}^2, \hat{\lambda}_{Z,h}(s) = \frac{\sum_{j=1}^{n} \frac{1}{h^2} K\left(\frac{s-z_j}{h}\right)}{\int_D \frac{1}{h^2} K\left(\frac{s-u}{h}\right) \nu(du)}$$

$$= \frac{\sum_{j=1}^{n} \frac{1}{h^2} K\left(\frac{s-z_j}{h}\right)}{p_h(s)}$$

Kernel intensity estimator

Edge correction:

Kernel intensity estimator

Edge correction:

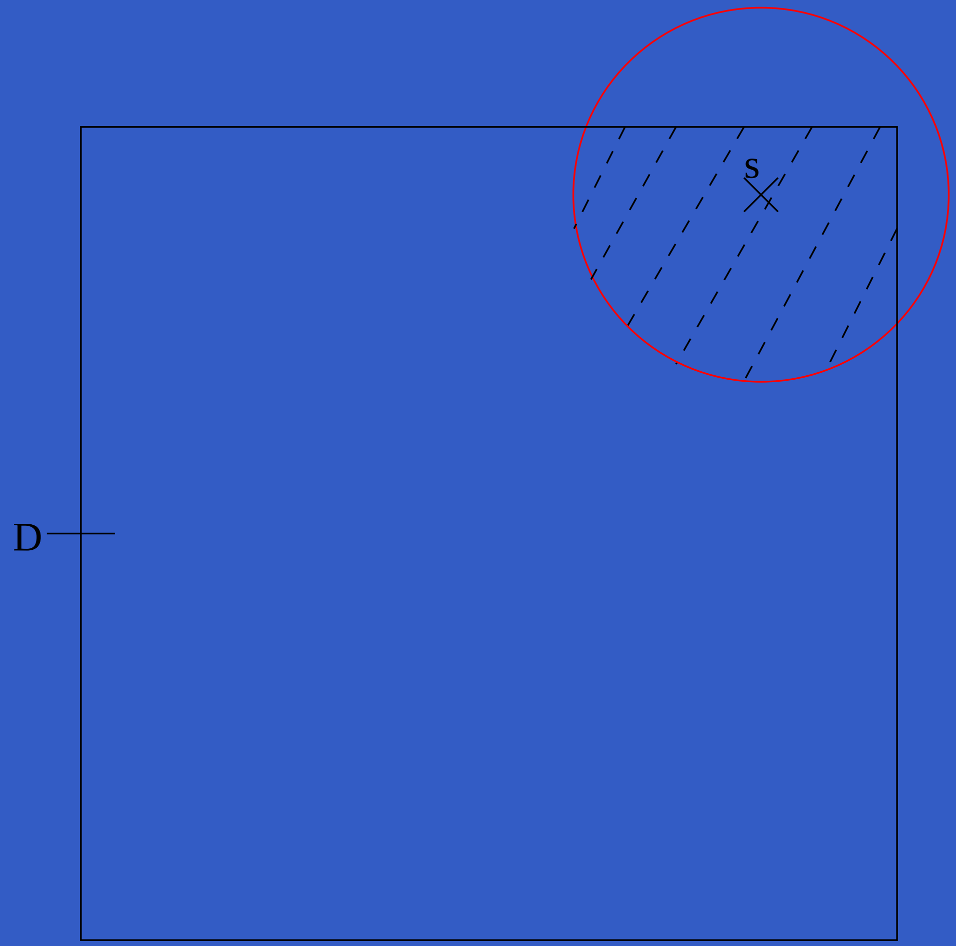

Deconvolution method

Deconvolution method

- Assume $\forall t \in \mathbb{R}^2, |\mathcal{F}(g)(t)| > 0.$

Deconvolution method

- Assume $\forall t \in \mathbb{R}^2, |\mathcal{F}(g)(t)| > 0$.
-

$$
\begin{aligned}
& z_i = y_i + \epsilon_i, \quad i = 1, \cdots, n \\
\Rightarrow \; & \lambda_Z = \lambda_Y * g \\
\Rightarrow \; & \mathcal{F}(\lambda_Z)(.) = \mathcal{F}(\lambda_Y)(.)\ \mathcal{F}(g)(.) \\
\Rightarrow \; & \mathcal{F}(\lambda_Y)(.) = \mathcal{F}(\lambda_Z)(.)/\mathcal{F}(g)(.) \\
\Rightarrow \; & \lambda_Y = \mathcal{F}^{-1}\big(\mathcal{F}(\lambda_Z)(.)/\mathcal{F}(g)(.)\big)
\end{aligned}
$$

Deconvolution kernel estimators

Deconvolution kernel estimators

- No edge-correction:

Deconvolution kernel estimators

- No edge-correction:

$$\lambda^*_{Y,h}(s) = \sum_{j=1}^{n} \frac{1}{(2\pi)^2} \int_{\mathbb{R}^2} e^{is't} \Big\{ \int_{\mathbb{R}^2} e^{-it'z} \frac{1}{h^2} K\big(\frac{z - z_j}{h}\big) \nu(dz)/\mathcal{F}(g)(t) \Big\} \nu(dt)$$

$$= \sum_{j=1}^{n} \frac{1}{h^2} K^*_h\Big(\frac{s - z_j}{h}\Big),$$

where $K^*_h(t) = \frac{1}{(2\pi)^2} \int_{\mathbb{R}^2} e^{it'y} \mathcal{F}(K)(y)/\mathcal{F}(g)(y/h) dy$.

Deconvolution kernel estimators

Deconvolution kernel estimators

- A priori edge-correction:

Deconvolution kernel estimators

- A priori edge-correction:

$$\hat{\lambda}_{Y,h}(s) = \mathcal{F}^{-1}\Big(\mathcal{F}(\hat{\lambda}_{Z,h})(t)/\mathcal{F}(g)(t)\Big)(s)$$
$$= \sum_{j=1}^{n} \frac{1}{(2\pi)^2} \int_{\mathbb{R}^2} e^{is't} \Big\{ \int_{G_h} \frac{e^{-it'z} \frac{1}{h^2} K\left(\frac{z-z_j}{h}\right)}{p_h(z)} \nu(dz)/\mathcal{F}(g)(t) \Big\} \nu(dt).$$

Deconvolution kernel estimators

Deconvolution kernel estimators

- A posteriori edge-correction:

Deconvolution kernel estimators

- A posteriori edge-correction:

$$\lambda^{**}_{Y,h}(s) = \frac{\lambda^{*}_{Y,h}(s)}{p^{*}_{h}(s)}.$$

The asymptotic study

The asymptotic study

Conclusions:

The asymptotic study

Conclusions:

- No estimator is asymptotically unbiased.

The asymptotic study

Conclusions:

- No estimator is asymptotically unbiased.
- We choose:

$$\lambda^{**}_{Y,h}(s) = \frac{\sum_{j=1}^{n} \frac{1}{h^2} K^*_h\left(\frac{s-z_j}{h}\right)}{\int_D \frac{1}{h^2} K^*_h\left(\frac{s-u}{h}\right)\nu(du)}, \forall s \in G'_h.$$

The asymptotic study

Conclusions:

- No estimator is asymptotically unbiased.
- We choose:

$$\lambda^{**}_{Y,h}(s) = \frac{\sum_{j=1}^{n} \frac{1}{h^2} K^*_h\left(\frac{s-z_j}{h}\right)}{\int_D \frac{1}{h^2} K^*_h\left(\frac{s-u}{h}\right)\nu(du)}, \forall s \in G'_h.$$

• asymptotically unbiased if homogeneous Poisson process,

The asymptotic study

Conclusions:

- No estimator is asymptotically unbiased.
- We choose:

$$\lambda^{**}_{Y,h}(s) = \frac{\sum_{j=1}^{n} \frac{1}{h^2} K_h^*\left(\frac{s-z_j}{h}\right)}{\int_D \frac{1}{h^2} K_h^*\left(\frac{s-u}{h}\right) \nu(du)}, \forall s \in G'_h.$$

• asymptotically unbiased if homogeneous Poisson process,
• reduces to Diggle estimator when no measurement error.

The bandwidth selection

The bandwidth selection

Adaptation of the gaussian reference rule to the bidimensional noisy case.

A band-limited kernel

A band-limited kernel

$$K_0(t) = \frac{48}{\pi} \frac{t^3 \cos(t) - 6t^2 \sin(t) + 15 \sin(t) - 15t \cos(t)}{t^7}$$

A band-limited kernel

$$K_0(t) = \frac{48}{\pi} \frac{t^3 \cos(t) - 6t^2 \sin(t) + 15 \sin(t) - 15t \cos(t)}{t^7}$$

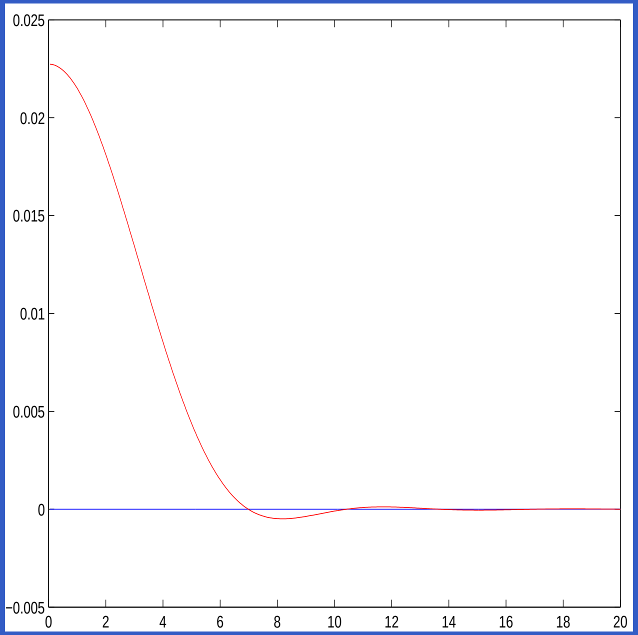

Figure 3: Profile of the kernel K_0

The Fourier transforms

The Fourier transforms

- $\mathcal{F}(K)(t) = (1 - t_1^2)^3 (1 - t_2^2)^3 \mathbb{1}_{[-1,1]^2}(t).$

The Fourier transforms

- $\mathcal{F}(K)(t) = (1 - t_1^2)^3(1 - t_2^2)^3 \mathbb{1}_{[-1,1]^2}(t).$
- $\mathcal{F}(g)$ usually explicit.

The Fourier transforms

- $\mathcal{F}(K)(t) = (1 - t_1^2)^3 (1 - t_2^2)^3 \mathbb{1}_{[-1,1]^2}(t).$
- $\mathcal{F}(g)$ usually explicit.
- Inverse Fourier transforms obtained by a numerical Simpson procedure

A simulation study

A simulation study

- $\{y_i, i = 1, \cdots, n\}$ from an inhomogeneous P.P with intensity
$\lambda_Y(s) = C\left[1 + 0.7\cos\left(2\pi(||s|| - 0.5)\right)\right].$

A simulation study

- $\{y_i, i = 1, \cdots, n\}$ from an inhomogeneous P.P with intensity
$$\lambda_Y(s) = C\left[1 + 0.7\cos\left(2\pi(||s|| - 0.5)\right)\right].$$

- $\{\epsilon_i, i = 1, \cdots, n\}$ i.i.d. $\sim g$.

A simulation study

- $\{y_i, i = 1, \cdots, n\}$ from an inhomogeneous P.P with intensity
$\lambda_Y(s) = C\left[1 + 0.7\cos\left(2\pi(||s|| - 0.5)\right)\right].$
- $\{\epsilon_i, i = 1, \cdots, n\}$ i.i.d. $\sim g$.
- $z_i = y_i + \epsilon_i, \quad i = 1, \cdots, n$

A simulation study

A simulation study

Denote

A simulation study

Denote

$$ISE = \int_{[0,1]^2} \left(\hat{\lambda}_{Z,h_{opt}} - \lambda_Y(s)\right)^2 \nu(ds)$$

A simulation study

Denote

$$ISE = \int_{[0,1]^2} \left(\hat{\lambda}_{Z,h_{opt}} - \lambda_Y(s)\right)^2 \nu(ds)$$

$$ISE^* = \int_{[0,1]^2} \left(\lambda^*_{Y,h^*}(s) - \lambda_Y(s)\right)^2 \nu(ds)$$

A simulation study

Denote

$$ISE = \int_{[0,1]^2} \left(\hat{\lambda}_{Z,h_{opt}} - \lambda_Y(s)\right)^2 \nu(ds)$$

$$ISE^* = \int_{[0,1]^2} \left(\lambda^*_{Y,h^*}(s) - \lambda_Y(s)\right)^2 \nu(ds)$$

$$ISE^{**} = \int_{[0,1]^2} \left(\lambda^{**}_{Y,h^*}(s) - \lambda_Y(s)\right)^2 \nu(ds).$$

A simulation study

A simulation study

Table 3: Gaussian error, σ=0.02

	ISE	ISE^*	ISE^{**}
1st quartile ($*10^3$)	1.0600	1.6745	0.9038
median ($*10^3$)	1.3939	1.9613	1.0279
3rd quartile ($*10^3$)	1.5899	2.2432	1.3158

A simulation study

Table 5: Gaussian error, σ=0.02

	ISE	ISE^*	ISE^{**}
1st quartile ($*10^3$)	1.0600	1.6745	0.9038
median ($*10^3$)	1.3939	1.9613	1.0279
3rd quartile ($*10^3$)	1.5899	2.2432	1.3158

Table 6: Gaussian error, σ=0.05

	ISE	ISE^*	ISE^{**}
1st quartile ($*10^3$)	0.8185	1.4153	0.6655
median ($*10^3$)	1.2474	1.7199	0.9298
3rd quartile ($*10^3$)	1.5281	1.8908	1.2138

A simulation study

A simulation study

Table 9: Laplace error, σ=0.02

	ISE	ISE^{*}	ISE^{**}
1st quartile ($*10^3$)	1.0444	1.4676	0.8274
median ($*10^3$)	1.4129	1.7275	1.0025
3rd quartile ($*10^3$)	2.1357	1.9753	1.2334

A simulation study

Table 11: Laplace error, σ=0.02

	ISE	ISE^*	ISE^{**}
1st quartile ($*10^3$)	1.0444	1.4676	0.8274
median ($*10^3$)	1.4129	1.7275	1.0025
3rd quartile ($*10^3$)	2.1357	1.9753	1.2334

Table 12: Laplace error, σ=0.05

	ISE	ISE^*	ISE^{**}
1st quartile ($*10^3$)	0.7869	1.1814	0.7689
median ($*10^3$)	1.4859	1.4223	1.1308
3rd quartile ($*10^3$)	2.0375	1.5114	1.4210

A simulation study

A simulation study

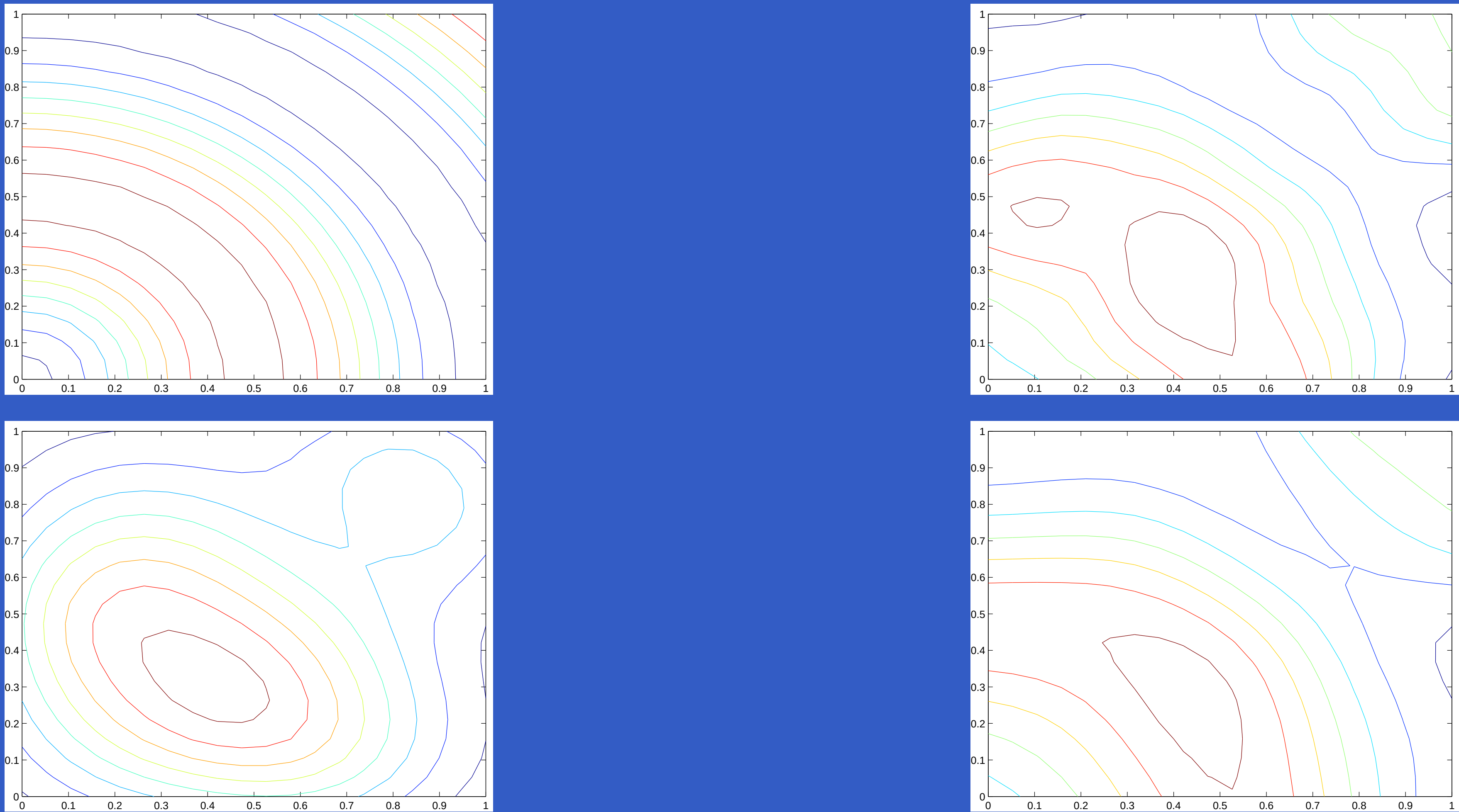

Figure 3 : Up-left figure: Contours of λ_Y. Up-right fig ure: Contours of $\hat{\lambda}_{Z,h_{opt}}$. Down-left figure: Contours of λ^*_{Y,h^*} Down-right figure: Contours of λ^{**}_{Y,h^*}